Analysis On Surface Enhanced Infrared Absorption Characteristics of Multi-Resonance Optical Antenna

Ruiqian Zhang*

Department of physics, The University of Hong Kong, Hong Kong, China

* Corresponding Author Email: zrqian@connect.hku.hk

Abstract. Infrared spectroscopy is an important detection technique. Because each functional group of different molecules has a fixed vibration mode, the molecules can be detected by infrared spectroscopy in the mid-infrared region. Metal nano-optical antennas can be used to construct high-sensitive sensors to detect different molecules. A structure with multi-band plasmon resonance is designed, which is composed of one gold nanorod and two symmetrical opening frames in order to detect the different target molecules simultaneously. In this study, the surface electric field distribution of the optical antennas is simulated by using finite difference time domain method (FDTD). In addition, the effects of the optical antenna structure on the surface enhanced infrared absorption (SEIRA) characteristics of the antenna are investigated. The different modes can be coupled, which brings new plasmon resonance peaks. It has been analyzed by the localized surface plasmons theory. These results provide a theoretical reference for the application of the new infrared sensing technology and shed light on guiding further exploration of infrared detectors.

Keywords: The surface enhances infrared absorption (SEIRA); localized surface plasmons theory; nanostructure; multi resonance.

1. Introduction

Mid-infrared spectral means the wavelengths located at 2μm to 20 μm, which can demonstrate characteristics of different molecules. The functional groups which constitute different molecules all have corresponding vibration modes. Different vibration periods correspond to different energy levels, and many information such as components and structure of molecules can be reflected by different energy levels [1].To enable high-sensitive molecular detection in nanodevices, various optical nano sensors have been studied, including the plasmonic nanoantenna [2], the fully dielectric metasurface [3], and the photon-sup-chip waveguide device [4]. Since the combination of infrared spectral vibration characteristics and the electric field enhancement induced by local surface plasmon resonance (LSPR), high sensitivity detection can be achieved, surface-enhanced infrared absorption based on LSPR has widely applications in many fields.

Near-field enhancement of metal micro-nano structures is one of its important optical properties with practical value. Absorption or emission spectral will be produced when molecules transition between different vibrational levels. Local surface plasmon can be used to enhance infrared signals on the antenna surface. Plasma resonance occurs when the surface of the metal micro-nano structure is irradiated by incident light. The electric transfer and collective oscillation will occur at specific positions of micro-nano structures. When detecting the electric and magnetic field strength in this area, it is found that both two fields can be enhanced. Changing the relevant parameters of the micro-nano structure allows the wavelength of local surface plasmon resonance to be accurately tuned over a large range. Thereore, it will targeted scatter and absorb different incident light at different wavelengths. By adjusting the structural parameters of the nanoantenna, the resonance wavelength can be changed. On this basis, the local electric field can resonant with the specific molecular functional group and absorb the light of the corresponding wavelength. Using infrared spectroscopy can achieve the purpose of accurate and efficient identification and detection of molecules [1]. The work of Novotny shows that one-dimensional nano rod, which produce plasmon resonance along the long axis when excited by the incident light field, can produce a resonance peak. The plasmon resonance wavelength is correlated with parameters such as material length:

$$\lambda_{eff} = \frac{2L}{m} + na_1 + na_2 \quad (1)$$

Where L is the length of the antenna, m is the number of vibration modes, n is the refractive index of the surrounding environment, a1 and a2 are related to the properties, the cross-section area, and the incident wave phase of the material. The resonance wavelength can be roughly calculated through this formula [1]. The geometry of one-dimensional rod nanoantenna is usually designed to realize single resonance mode. A single metal nano-rod under incident light is excited with an pronounced plasmon resonance peak, which provides a strong electromagnetic field. The position of the resonance peak can be adjusted by changing the parameters such as the length and thickness of the individual nano-rods to match the molecular vibration mode, so as to probe the specified molecules. However, because the one-dimensional rod nanostructure can only tune the resonance wavelength and cannot increase the number of resonance peaks, the complex and combined nanostructures should be selected to provide different resonance peak positions at different wavelengths. By tuning the resonance wavelength, the nanostructure can be coupled to each other, producing some related effects, such as the Fano resonance. When multiple nanostructures are combined in various ways, multiple plasmon resonance modes can be coupled to produce more Fano linear types, and accurately regulate the relevant spectra, so they can meet the application needs at multiple resonance wavelengths [5].

In the quantum domain, In 1961, Fano found that the inelastic scattering between electrons and helium creates asymmetric scattering lines near the energy of the self-ionization [6]. When comparing this concept to surface-enhanced infrared absorption properties, two different resonance modes may appear in some complex metal nanostructures. One is the broadband superradiation mode, which can be seen as an analogue to the continuous state in the field of atomic physics. This is a bright mode; Another is narrow-band subradiation mode, which can be comparable to the excited energy levels produced by discrete states in the field of atomic physics. This is a dark mode. Tuning the frequencies of these two resonance modes, the drastic mutual coupling effect will happen when they overlap with each other. Beisdes, an asymmetric linear type appears in the scattering, absorption, or extinction spectra of metal nanostructures. A Fano resonance is generated at this time. The Fano linear type is related to the structural parameters of the system as well as to the electromagnetic parameters of the ambient medium, so that many artificial plasmas have been proposed to produce distinct Fano resonances. The properties associated with the Fano resonance enable various potential applications, and nowadays, the Fano resonance has a wide range of photon applications.

In order to detect different kinds of molecules at the same time, a multi-band resonance complex combination of optical antenna structure has been designed. The finite time domain difference (FDTD) method simulation waas used to analysis the impact of optical antenna size, shape, combination mode and other parameters on its multi-band resonance.

2. Methodology

Based on the simulation of finite difference time domain (FDTD) method, the influence of the size, shape and combination mode of the optical antenna on the multi-band resonance is studied. The finite time domain difference method (FDTD) is the calculation method of solving the complex structure and the regional Maxwell equations. Before performing the calculation, discrete time and space first use a discrete grid to differentiate the calculated electromagnetic fields and complex structures, solving a set of Maxwell equations in each differentiated grid. The near-field and far-field properties of many materials and type nanostructures under incident light can be analyzed by FDTD. After obtaining the result of time-domain difference, the frequency-domain information contained in the same region can also be obtained.

Research with FDTD methods is more convenient and efficient in electromagnetism and optics, so the applications in these related fields have great advantages. When solving the Maxwell equations in the complex geometry and regions during the simulation calculation, the FDTD method is first

used to discretize the regions and structures, and solve the Maxwell equations in the non-magnetic materials in the discrete regions respectively:

$$\nabla \times \boldsymbol{E} = -\frac{\partial \boldsymbol{B}}{\partial \boldsymbol{t}} - \boldsymbol{J} \tag{2}$$

$$\nabla \times \boldsymbol{H} = \frac{\partial \boldsymbol{D}}{\partial \boldsymbol{t}} + \boldsymbol{J}^{*} \tag{3}$$

$$\nabla \cdot \boldsymbol{B} = \mathbf{0} \tag{4}$$

$$\nabla \cdot \boldsymbol{D} = \boldsymbol{\rho} \tag{5}$$

The vector $\boldsymbol{E}$ is electric field strength, $\boldsymbol{H}$ is magnetic field strength, $\boldsymbol{D}$ is electric displacement vector, $\boldsymbol{B}$ is magnetic induction strength; $\boldsymbol{J}$ * is current density, $\boldsymbol{J}$ is magnetic current density; $\boldsymbol{\rho}$ is charge density. Moreover, if studied in a three-dimensional space, then Maxwell's equation has six electromagnetic field components. In the spatial right-angle coordinates, assuming that the selected object in the z axis direction, and the electric field and magnetic field are independent of the z axis direction, then the Maxwell equation into two non-interrelated equations, solved in the x-y plane, thus get the correlation equations of TE wave and TM wave Ex, Ey and Hz, and Hx, Hy and Ez components for TM equation [7]:

$$\frac{\partial E_Z}{\partial y} - \frac{\partial E_y}{\partial z} = -\mu_0 \frac{\partial H_y}{\partial t} \tag{6}$$

$$\frac{\partial E_x}{\partial z} - \frac{\partial E_z}{\partial x} = -\mu_0 \frac{\partial H_x}{\partial t} \tag{7}$$

$$\frac{\partial E_y}{\partial x} - \frac{\partial E_x}{\partial y} = -\mu_0 \frac{\partial H_z}{\partial t} \tag{8}$$

$$\frac{\partial H_z}{\partial y} - \frac{\partial H_y}{\partial z} = \varepsilon \frac{\partial E_x}{\partial t} \tag{9}$$

$$\frac{\partial H_x}{\partial z} - \frac{\partial H_z}{\partial x} = \varepsilon \frac{\partial E_y}{\partial t} \tag{10}$$

$$\frac{\partial H_y}{\partial x} - \frac{\partial H_x}{\partial y} = \varepsilon \frac{\partial E_z}{\partial t} \tag{11}$$

Yee proposed in the case of three dimensions can divide space cube, the sampling point of six electromagnetic field components in the space cube edge and the heart. with the distribution of electromagnetic field component method, can do the Maxwell equation center difference approximate, so can more accurately present the electromagnetic wave propagation [8].

3. Results & Discussion

3.1. SEIRA of the gold rod and gold opening frame

Combination structure is complex. In order to clearly study the complex structure surface enhanced infrared absorption mechanism, firstly, the complex structure is divided into a single metal nano-rod, a single opening half frame and simple unit structure. These simulations were performed separately using the FDTD method. After analysing the results, the complex structure can be studied. The length of gold nano rod is L_d, d1=170nm is the width, and d=55nm is the thickness. The length, width, and height of the substrate are P_y=3.5 m, P_x=3.5 m, and P_z=1 m, respectively. The incident light is the full-field scattering field plane wave. The incident light polarization direction is along the y-axis, and the incident direction acts vertically to the gold nanostructure along the z-axis. The size of the FDTD simulation region was set as 3000 nm×3300nm×700nm, with a calculated grid accuracy of 5nm. The boundary condition is set as perfectly matched layer (PML). The effect of the peak and the strength of the gold nanobrod was investigated. The width d_1=170nm and the thickness d=55nm of the gold nano rod is kept unchanged, the length L_d changes from 2.2μm and increase the rod length by 50nm each time. The field enhancement result is expressed by the ratio of the enhanced electric field to the

incident optical electric field intensity in $|E/E_0|$, where E is the electric field intensity of the detection point near the gold nano-rod when the incident light enters vertically onto the CaF_2 substrate and E_0 is the electric field intensity of the incident light. The simulation results are shown in Fig. 1. The electric field profile at the gold nanorod length of 2.5μm is shown in Fig. 1 (c). The electric field strength is strongest at the four tips of the gold nanorods, and this region is a hot spot region. As shown in Fig. 1(d), gold nanorods exhibit typical optical antenna features, the plasma resonance wavelength is redshifted. It was changed from 6.1μm to 6.6μm. Fig. 1(e) show that the figures $|E/E_0|$ of single gold nano-rod resonance are proportional to the length of the gold nanorod, and meet the linear relationship, the rule as shown in the Eq. (1). Keeping the transverse side length of the frame L_x=900nm, the length of two arms L_y=900nm, and the thickness d=55nm during the simulation, the substrate parameters are still consistent with those described in the previous section.

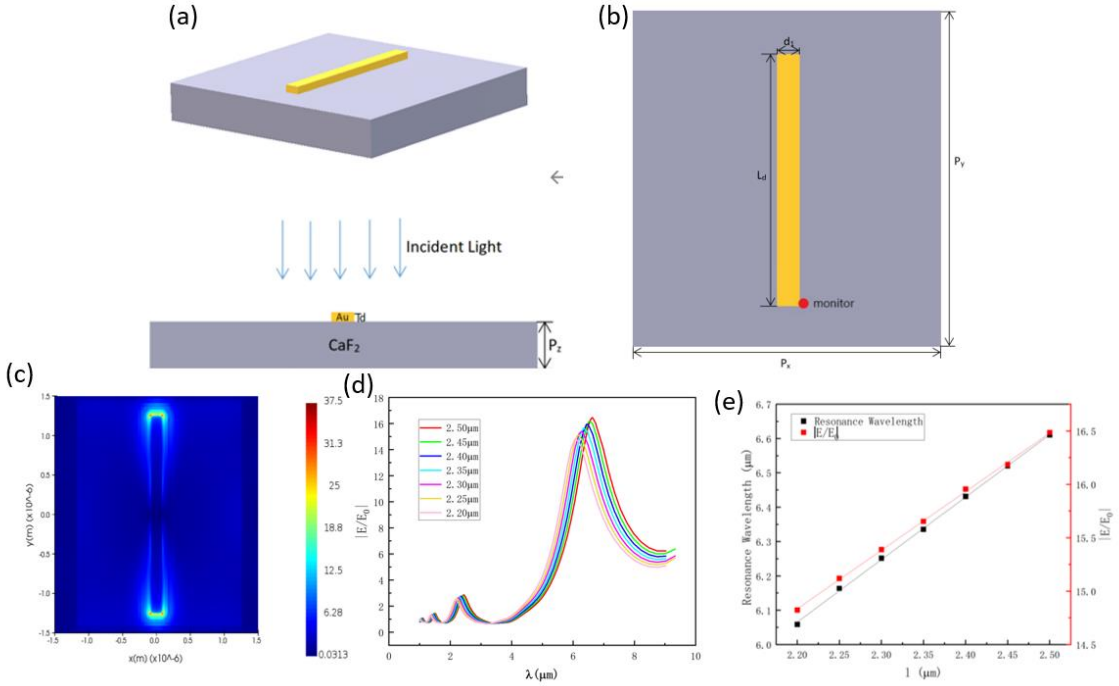

Fig. 1 (a) Diagram of gold nanorod structure and x-z direction; (b) diagram of the gold nanorods in the x-y direction and the position of the monitors; (c)Electric field profile of gold nanorods under incident light excitation); (d)Plot of the gold nanorod field strength ratio with different lengths Ld; (e)Resonant peak positions and field strength ratios corresponding to gold nanorods of different lengths.

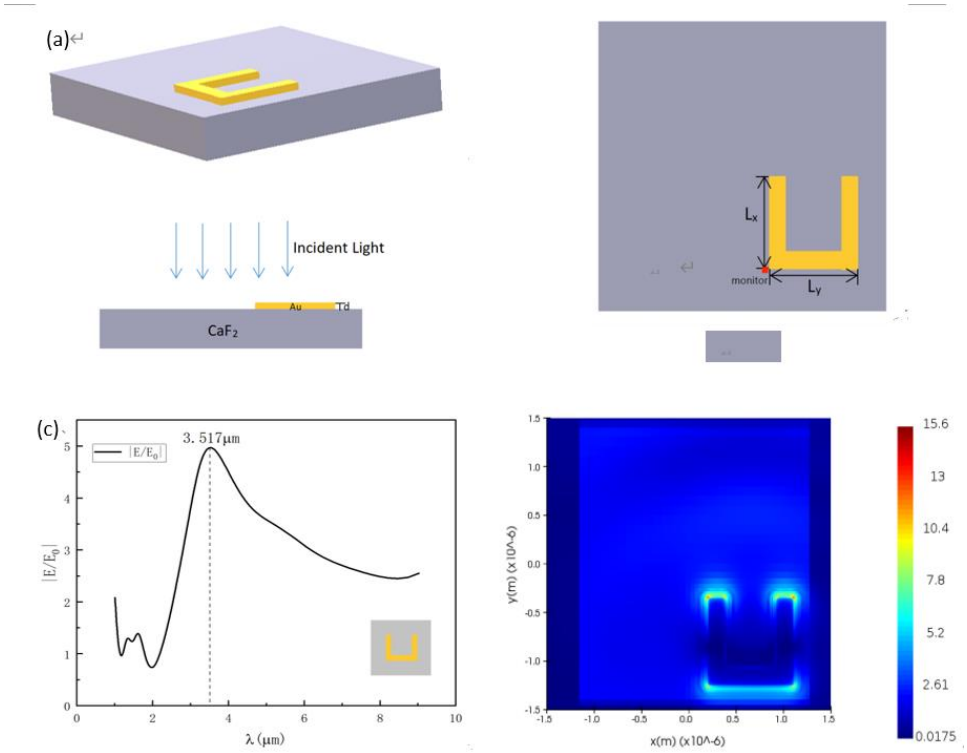

Fig. 2 (a) Diagram of gold opening frame and x-z direction; (b) diagram of the gold opening frame in the x-y direction and the location of the monitoring points; and (c) the plot of the field intensity ratio changing with the incident light wavelength and the electric field distribution of the opening frame and the electric field vector under the incident light excitation.

As can be seen from Fig. 2, the resonance wavelength of a single gold frame is λ=3.517 μm. The upper part of the overall electric field of the frame is positive and the lower part is negative, and the overall excited longitudinal dipole moment is positive and negative, which is comparable to the electric dipole moment excited by a single gold nanorod.

3.2. SEIRA of the combined structure

The range of the plasmon resonances wavelength of a single structure is too narrow to detect multiple molecules at different frequencies simultaneously. To compensate for this deficiency, the combined structure is designed to realize the multi-resonance mode of the optical antenna. First, a simple combination of the two cell structures, that is, a gold nanorod and a gold opening half-frame, is shown in Fig. 3.

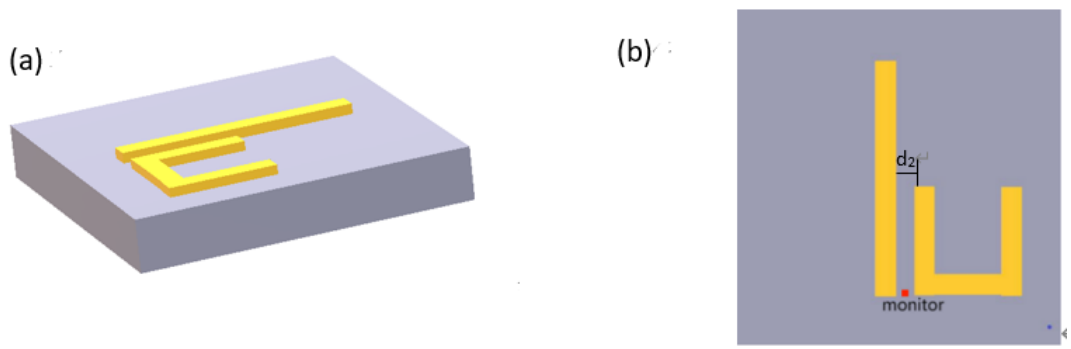

Fig. 3 (a) Diagram of the combined structure of nanorod and single opening frame and (b) diagram of x-y direction structure and position of monitor.

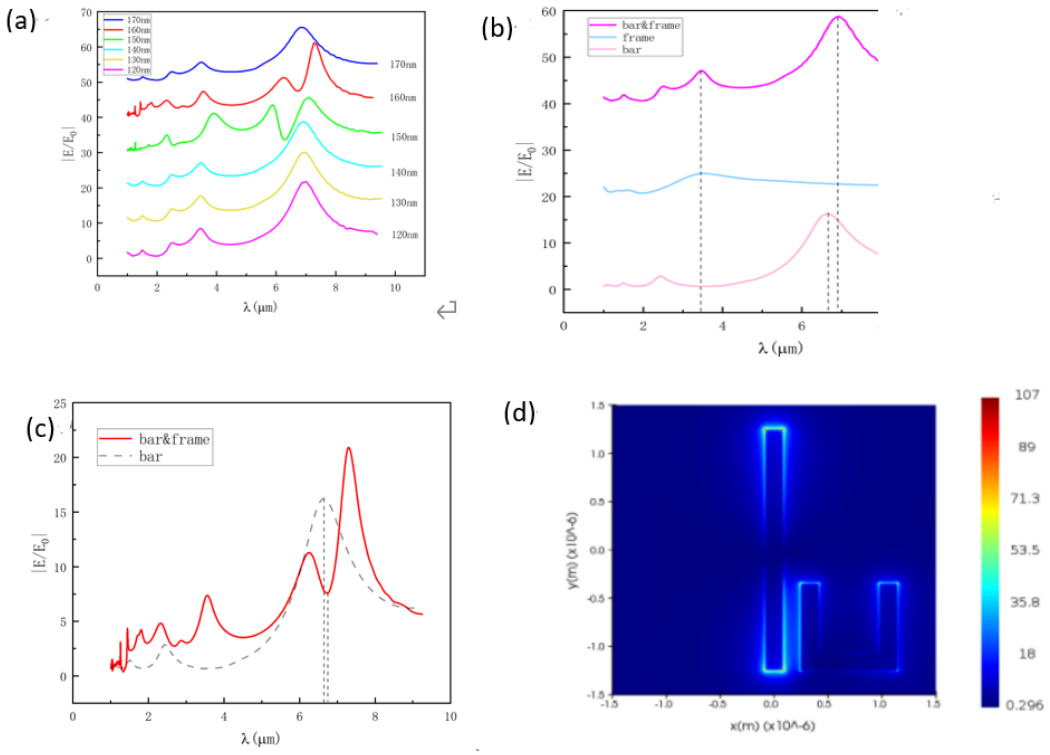

Fig. 4 (a) Diagram of $|E/E_0|$ corresponding to different gaps between the gold nanorods and the opening frame along with the wavelength change of the incident light;(b) Comparison diagram of the change relationship of $|E/E_0|$ of a single gold nanorood, a single opening box, a brodand an opening frame at a gap of 120nm; (c) Comparison diagram of the $|E/E_0|$ changing with incident light wavelength between a brodand an open box gap 160nm in Fano resonance (red curve) and a single brodfield strength ratio 2.5 m long (gray dashed line); (d) Corresponding electric field profile and electric field vector distribution at the Fano resonance valley (6.779 m) when the brodand the opening box gap is 160nm.

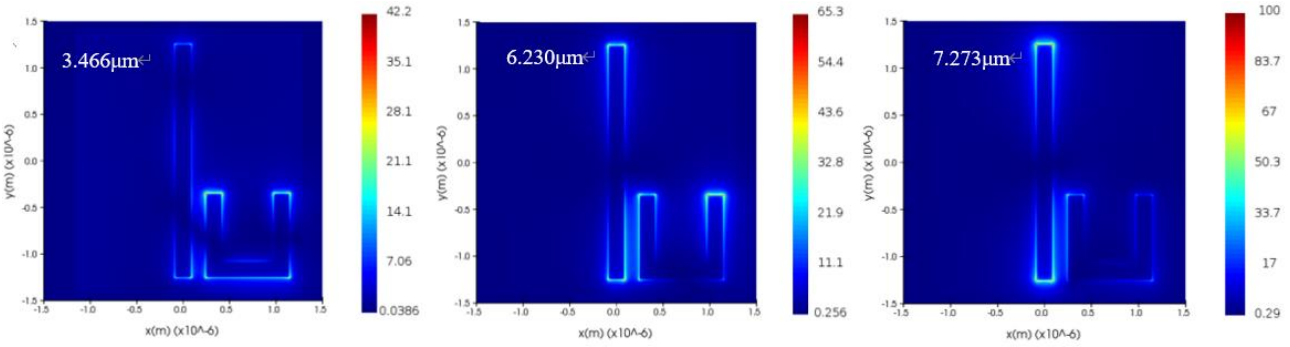

Fig. 5 Electric field profile and electric field vector distribution corresponding to the three resonance wavelengths (3.541μm, 6.230μm, 7.273μm) between the rod and the opening frame gap at 160nm.

Taking nitrate ions as one of the target probes for multi-molecule detection. According to the known experimental results, the characteristic wavelength of nitrate ions is 7.26 μm, which needs to regulate the structure of the plasma resonance peak of around 7.26 μm. Gold nanorod with length L_d=2.5μm, width d_1=170nm, thickness d=55nm, and gold opening frame with length of arms L_x=L_y=900nm, width d_1=170nm, thickness d=55nm have been selected. The opening frame was placed on the right side of the gold nanorod, and the gap between the gold nanorood and the opening frame was varied at every 10nm interval between 120 and 170 nm, and it was simulated separately, and the results are shown in Fig. 4.

For the cause of resonance peaks (seen from Fig. 5), there are two plasma resonance peaks at around 3.5μm and around 6.9μm at the gap of 120nm, 130nm, 140nm and 170nm, respectively. Taking the gap of 120nm as an example, although the far right-hand plasma resonance peak has a certain redshift relative to the individual gold nanorods, the redshift distance is small, and the wavelength position of the two resonance peaks almost overlap with the individual gold opening frame structure and the individual gold nanorods resonance peak position, respectively. At the same time, the electric field distribution of the combined structure at the resonance peak is further analyzed. The ratio of $|E/E_0|$ and the incident light field intensity of the enhanced electric field and the incident light field intensity of the combined structure are shown in Fig. 4(b). When the incident light wavelength is around the position $\lambda = 3.5\mu m$ of the first resonance peak, the right opening box in the combination structure is excited with a strong field enhancement mode, while the gold nanorods is only excited by a very weak field enhancement mode, and when the incident light wavelength is around position $\lambda = 6.9$ μm. In this case, the two resonance peaks are generated by the gold opening frame and the gold nanorod excitation, respectively. However, the Fano resonance can be observed at the gaps 150nm and 160nm, and the main peak at $\lambda = 6.9\mu m$, as seen in Fig. 4(c), the position of the cleave valley almost overlaps with the ionization resonant position of a single gold nanorod. According to the theory of coupling of the plasmon resonance models, when there is a suitable gap between the two nanometer structures, the middle gold nanorods and next to the gold opening half frame structure may have a strong near-field coupling effect, the middle gold nanorods resonance mode and the right gold opening box resonance mode will be coupled [9], coupling will lead to a new resonance mode, form the bright mode in the Fano resonance and dark mode, the interaction of the two modes will produce asymmetric Fano resonance linear type. When the gap between the gold nanorod and the right opening frame is 150nm and 160nm, The Fano Resonance Valley is near 6.285μm and 6.751μm, respectively, The largest plasma resonance peaks were at 7.105μm and 7.273μm, respectively, $\lambda = 3.541$ μm, $\lambda = 6.230$ μm and nitrate ion ($\lambda = 7.26\mu m$), substituted benzene molecules ($\lambda = 3.30\mu m$), $\lambda = 6.230\mu m$ and $\lambda = 7.273\mu m$), respectively.

After studying the combined structures of single gold nanorod, single gold opening frame and the combinaton of one rod and one opening frame, the electric field enhancement properties and near-field coupling effects of the complex combined structures of gold nanorod and symmetrically placed gold opening frame are studied. This complex combined structure can be viewed as a multi-resonance nanoantenna plasma sensor based on plasmon resonance and light-dark coupling that can produce multiple resonance peaks in the mid-infrared fingerprint region. The length, width and thickness of the middle gold nanorod and the gold opening frame on both sides are still consistent with those in the previous section. 120~170nm adjusted the gap d2 of the gold nanorods and 170nm symmetrically to observe the change of the plasmon resonance peak.

When adjusting the gap between the gold nanorod and the opening frame to 120nm, observing the relative electric field intensity and the incident light wavelength found one more resonance peak than in the previous section of a gold nanorod and an opening frame, with a total of three resonance peaks. The results are presnetd in Fig. 6. As shown in Fig. 6 (c), when the electric field is aligned with the two longitudinal arms of the opening frame, the incident light polarization direction is along the y direction, the issocion resonance mode of the gold nanorods and the gold opening frame on both sides are coupled, producing a total of three resonance peaks. The corresponding electric field profiles at the three resonance peaks (3.438μm, 5.164μm, and 7.095μm), representing the two resonances caused by the coupling of gold nanorod and opening frames, respectively.

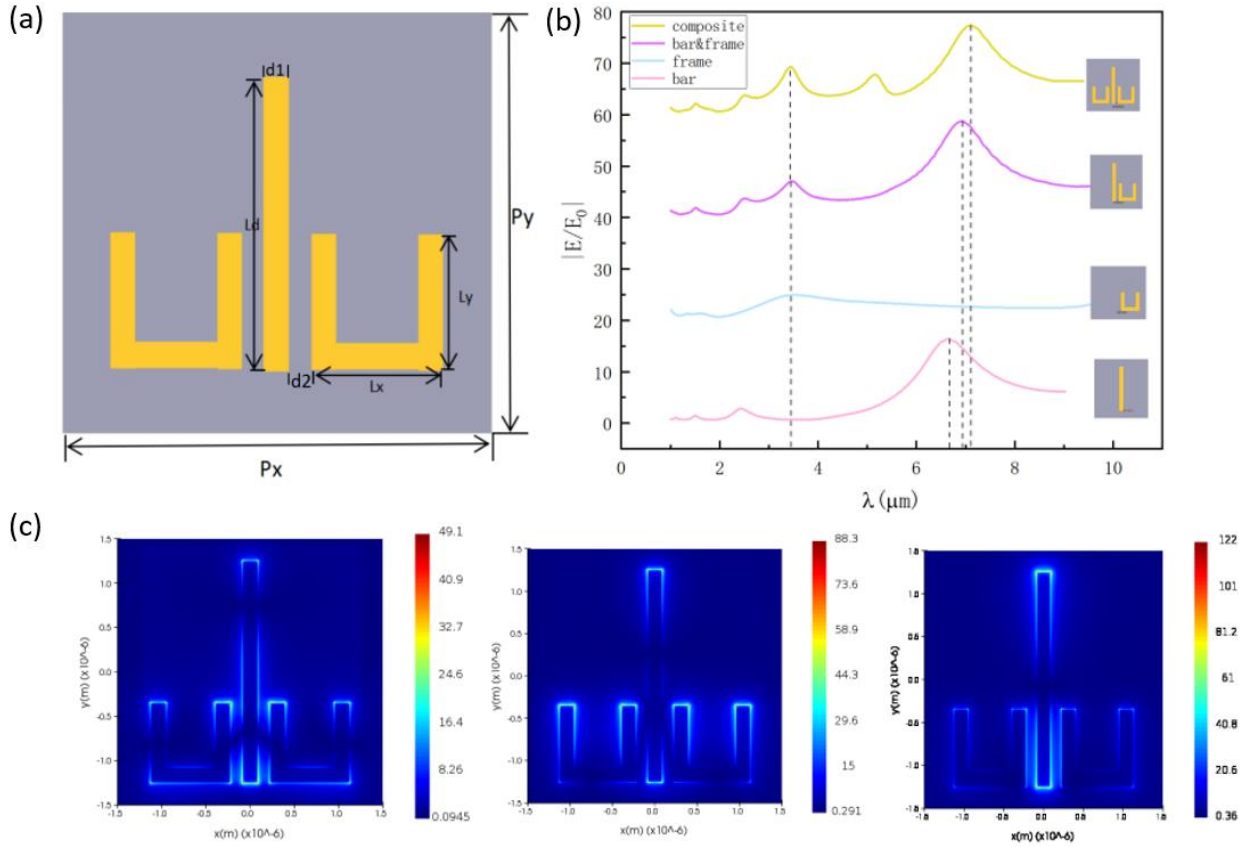

Fig. 6 (a) Diagram of the x-y direction of the complex combination structure. (b) Plot of the corresponding field strength ratio change with the incident light wavelength when a single gold nanorod, a single opening frame, a rod and an opening box gap 120nm, a complex combined structure rod and the opening frame gap 120nm. (c) Electric field profile map and electric field vector distribution map at the three resonance peaks of the gold nanorod and the bilateral opening frame gap of 120nm.

Seen in Fig. 7(a), when the gap is 150nm and 160nm, compared with the other gaps, The waveform changes more dramatically and there is a shoulder peak about 6.5 μm. So a Fano resonance may occur when the gap between the gold nanorods and the lateral open box is 150nm and 160nm . Because the two gold opening frames are symmetrically placed about the middle gold nanorod, the gap of 160nm were chosen to verify the generation of Fano resonance by setting monitoring points at different positions in the right gap. Different monitoring points were set up at the positions of 35nm, 45nm, 55nm, 70nm, 80nm, and 90nm from the gold nanorod in the right gap. The relation diagram of the field intensity ratio and the incident light wavelength, such as Fig7 (b), as can be seen, at 55nm from the gold nanorod, there is a Fano resonance linear type beginning to appear. The original plasma resonance peak at the incident light wavelength of 7.32μm was split into two peaks at around 6.7μm, the position of the Fano cleft valley almost overlapped with the resonance peak positions of individual gold nanorod. The overall linear type is changed from three resonance peaks to four resonance peaks.

The Fano resonance phenomenon can be explained by the theory of resonance modes coupled to each other. If the bright mode and the dark mode coupling matches at the same incident light wavelength, the plasma bright dark coupling can excite the new coupling modes. When multiple nanostructures are combined and the gap between different nanostructures is smaller than the incident light wavelength, their plasmon resonances are coupled to each other to form two new different resonance peaks [10]. It can be inferred that the Fano resonance here is caused by the mutual coupling of the bright and dark modes resulting from the interaction in the system. From the above results, the resonant modes of gold nanorods act as bright modes in the structures designed here. The dark mode is excited when the gold nanorods and two symmetric gold-opening frames are combined. Meanwhile, from Fig. 7 (c), one can infer the bright mode and the dark mode interaction formed between the

resonance modes of the three basic structures, so that the plasma resonance peak can split and form an asymmetric Fano type of line. On the one hand, the split peak can be generated through the Fano resonance, and the structure resonates in multiple bands to simultaneously identify and detect different types of molecules. On the other hand, this structure compensates for the small limitation of hot spot area in individual structures. The Fano resonance makes the relative electric field strength at the peak position of the plasma resonance peak somewhat enhanced when compared with the time when no Fano resonance occurs. Therefore, in the gap between the gold nanorods and the open frame, the sensitivity of molecular detection is improved, and it provides an effective theoretical basis for the application of related infrared detection sensor in practice.

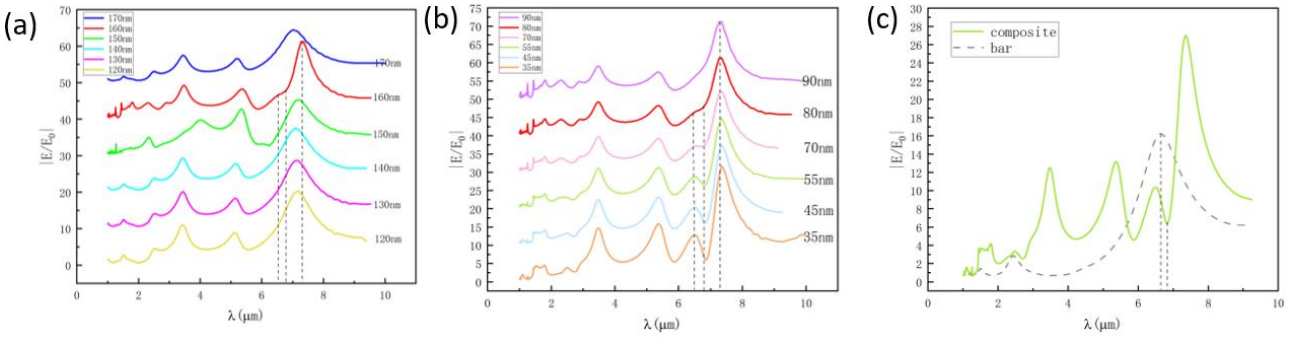

Fig. 7 (a) Plot of the corresponding field intensity ratio of the different gaps of the rod and the opening frames in complex combination structure along with the incident light wavelength change;(b) Adjust the monitor position of the gold nanorod and the opening box gap of 160nm, and the corresponding field intensity ratio of the six monitoring points changes with the wavelength of the incident light;(c) Comparison of field strength ratio change with incident light wavelength in Fano resonance at 160nm (green curve) and change of field strength ratio of a single rod with incident light wavelength at 2.5 μ m long (gray dashed line).

4. Limitations & Prospects

Based on the theoretical and simulation results presented here, further studies are expected on the complex combined nanostructure arrays designed in this paper. On the one hand, the array structure may produce multiple Fano resonance splitting peaks with a more narrow line width to further improve the sensitivity and accuracy of the probe. In addition, the molecular detection and identification can be expanded in a larger area, making the detection more convenient and efficient to meet the needs of specific micro-nano photonics.

5. Conclusion

In summary, this study discusses the surface enhanced infrared absorption characteristics of multi-resonance optical antenna. To be specific, this paper first introduces the research used including local surface equal distant excitation element, single resonance mode, multiple resonance mode and finite time domain difference method of basic theory. Based on the principle of local surface plasmon resonance and using limited time domain difference method simulation, the surface enhanced infrared absorption mechanism of a single gold nanorod, a single gold opening frame were investigated, respectively. By analyzing the simulation results of simple cell structures, complex combined nanostructures were further studied. Besides, the cause of multiband resonances of complex combined nanostructures were briefly explain, including the coupling of multiple modes and the generation of Fano resonances. The surface-enhanced infrared absorption characteristic of multi-resonance optical antennas has practical applications, and the resulting resonance peaks at multiple wavelengths of the incident light can identify and detect different molecules simultaneously, which provides an important theoretical background for highly sensitive infrared detectors.

References

[1] Li Nannan, Zhang Han, Wang Jianfang. Local surface enhance infrared absorption. Chinese Science: Physics, mechanics, Astronomy, 2019, 49(12): 26-39.(in Chinese)

[2] Hasan Dihan, et al. Dipolar resonance enhancement and magnetic resonance in cross-coupled bow-tie nanoantenna array by plasmonic cavity. Acs Photonics, 2015, 2.7: 890-898.

[3] Chang, Yuhua, et al. All-dielectric surface-enhanced infrared absorption-based gas sensor using guided resonance. ACS applied materials & interfaces 2018, 10.44: 38272-38279.

[4] Qiao Qifeng, et al. Applications of photonic crystal nanobeam cavities for sensing. Micromachines 2018, 9.11: 541.

[5] Li Aiyun, Zhang Xingfang, Liu Fengxu, et al. Fano resonance properties of symmetric nanorood trimer structures. Journal of Physics, 2019, 19.(in Chinese)

[6] Jin Yuerong, Chen Zhuo, Wang Zhenlin. Generation conditions for Fano resonances in an ordered array of metal micro-nano structures. Chinese science: Physical mechanics and astronomy, 2013.(in Chinese)

[7] Zeng Zheng, Liu Yiyang, and Wei Jianjun. Recent advances in surface-enhanced raman spectroscopy (SERS): Finite-difference time-domain (FDTD) method for SERS and sensing applications. TrAC Trends in Analytical Chemistry, 2016, 75: 162-173.

[8] Tan Wei, Yang Cun, Tang Jilong, et al. Study on the enhanced extinction properties of Au nanoantenna based on Time domain Finite difference method. Photon Journal, 2018 (5): 78-83.

[9] Fano Ugo. Effects of configuration interaction on intensities and phase shifts. Physical Review 1961, 124.6: 1866.

[10] Aouani Heykel, et al. Ultrasensitive broadband probing of molecular vibrational modes with multifrequency optical antennas. Acs Nano 2013, 7.1: 669-675.